ISSN 1674-1056
http://cpb.iphy.ac.cn
http://iopscience.iop.org/cpb
中国物理 B
Chinese Physics
中国物理 Chinese Physics B

Multistability and coexisting transient chaos in a simple memcapacitive system

Fu-Ping Wang(王富平), Fa-Qiang Wang(王发强)

Citation: Chin. Phys. B . 2020, 29(5): 058502 . **doi:** 10.1088/1674-1056/ab7e98
Journal homepage: http://cpb.iphy.ac.cn; http://iopscience.iop.org/cpb

What follows is a list of articles you may be interested in

Investigation of gate oxide traps effect on NAND flash memory by TCAD simulation

He-Kun Zhang(章合坤), Xuan Tian(田璇), Jun-Peng He(何俊鹏), Zhe Song(宋哲), Qian-Qian Yu(蔚倩倩), Liang Li(李靓), Ming Li(李明), Lian-Cheng Zhao(赵连城), Li-Ming Gao(高立明)

Chin. Phys. B . 2020, 29(3): 038501 . **doi:** 10.1088/1674-1056/ab695f

A new nonlinear oscillator with infinite number of coexisting hidden and self-excited attractors

Yan-Xia Tang(唐妍霞), Abdul Jalil M Khalaf, Karthikeyan Rajagopal, Viet-Thanh Pham, Sajad Jafari, Ye Tian(田野)

Chin. Phys. B . 2018, 27(4): 040502 . **doi:** 10.1088/1674-1056/27/4/040502

Parameter analysis of chaotic superlattice true random number source

Yan-Fei Liu(刘延飞), Dong-Dong Yang(杨东东), Hao Zheng(郑浩), Li-Xin Wang(汪立新)

Chin. Phys. B . 2017, 26(12): 120502 . **doi:** 10.1088/1674-1056/26/12/120502

Graphene resistive random memory–the promising memory device in next generation

Xue-Feng Wang(王雪峰), Hai-Ming Zhao(赵海明), Yi Yang(杨轶), Tian-Ling Ren(任天令)

Chin. Phys. B . 2017, 26(3): 038501 . **doi:** 10.1088/1674-1056/26/3/038501

Complex transitions between spike, burst or chaos synchronization states in coupled neurons with coexisting bursting patterns

Gu Hua-Guang, Chen Sheng-Gen, Li Yu-Ye

Chin. Phys. B . 2015, 24(5): 050505 . **doi:** 10.1088/1674-1056/24/5/050505

Multistability and coexisting transient chaos in a simple memcapacitive system*

Fu-Ping Wang(王富平) and Fa-Qiang Wang(王发强)†

State Key Laboratory of Electrical Insulation and Power Equipment, School of Electrical Engineering, Xi'an Jiaotong University, Xi'an 710049, *China*

(Received 6 January 2020; revised manuscript received 2 March 2020; accepted manuscript online 11 March 2020)

The self-excited attractors and hidden attractors in a memcapacitive system which has three elements are studied in this paper. The critical parameter of stable and unstable states is calculated by identifying the eigenvalues of Jacobian matrix. Besides, complex dynamical behaviors are investigated in the system, such as coexisting attractors, hidden attractors, coexisting bifurcation modes, intermittent chaos, and multistability. From the theoretical analyses and numerical simulations, it is found that there are four different kinds of transient transition behaviors in the memcapacitive system. Finally, field programmable gate array (FPGA) is used to implement the proposed chaotic system.

Keywords: memcapacitive system, multistability, coexisting attractors, transient transition behaviors

PACS: 85.25.Hv, 05.45.Pq **DOI:** 10.1088/1674-1056/ab7e98

1. Introduction

Over the past few decades, chaos has been studied by many researchers. The first chaotic system was founded by Lorenz in 1963.[1] Since then, various chaotic systems have been proposed, such as Rössler,[2] Chen,[3] Lü,[4] Chua,[5] and Liu systems.[6] All these chaotic systems are self-excited systems, which is a concept defined by Kuznetsov and Leonov.[7] Also, in this reference, they divided these chaotic attractors into two types, self-excited attractors and hidden attractors. For the hidden attractor, its definition is: the basin of attraction of hidden attractor will not connect with unstable equilibrium point.[8,9] But for the self-excited attractor, it results from an unstable equilibrium point.[10,11] Since then, many achievements have been obtained by researchers interested in hidden attractor chaotic system, such as the chaotic systems with no equilibrium point, with stable equilibrium points, with infinite number of equilibrium points. For example, Zhou presented a three-dimensional (3D) chaotic system without equilibrium point but can generate hidden attractors.[12] Pham introduced a nonlinear system with only one stable equilibrium point.[13] Sprott investigated the coexistence of point, period, and chaos in a chaotic system with stable equilibrium point.[14] Barati proposed chaotic system with curves of equilibrium points.[15]

In addition, under fixed parameters, different chaotic attractors in different initial conditions can be found in coexisting attractor systems, which is defined as multistability in chaotic systems. For example, Lai presented a four-dimensional (4D) chaotic system with different kinds of coexisting attractors, such as attractors with four limit cycles, single-scroll attractors, and double-scroll attractors.[16] Pham studied a chaotic system with coexisting attractors and without equilibrium point.[17] Different kinds of coexisting attractors can be found in Ref. [18], such as point attractors, hidden attractors, limit cycles, and hyperchaos. In addition, the most important characteristic of Ref. [19] is that it possesses an infinite number of equilibrium points in a six-element-memcapacitor-based circuit with coexisting attractors and extreme multistability. Yuan investigated nonlinear dynamics of coexisting attractors in a memcapacitive system with different starting conditions.[20] Hyperchaotic system with infinite equilibrium points and coexisting attractors in a memcapacitor oscillator is accomplished in Ref. [21]. The hyperchaotic system was implemented by field programmable gate array (FPGA).

Furthermore, in recent years, there has been an interest about the concept of transient transition behavior in academic circles. In a nonlinear system, transient transition behaviors are temporal evolutions before steady states. Transient transition behaviors can be more relevant than the steady states of the system in terms of the observation, modeling, prediction, and control of the system. As a result, transient transition behaviors are important to nonlinear systems such as physics, chemistry, biology, engineering, and economics. What is more, it is useful to study this subject because transient behaviors can arise in many fields: shimmy of the front wheels of motorcycles and airplanes,[22] a compass forced by a magnetic field,[23] lasers,[24] and electronic oscillators.[25] The phenomenon of transient transition behavior in the chaotic system could be divided into two types, transient chaos and transient period. On the one hand, transient chaos,[26,27] is a com-

*Project supported by the National Natural Science Foundation of China (Grant No. 51377124) and the Science Fund for New Star of Youth Science and Technology of Shaanxi Province, China (Grant No. 2016KJXX-40).

†Corresponding author. E-mail: faqwang@xjtu.edu.cn

© 2020 Chinese Physical Society and IOP Publishing Ltd

mon phenomenon, which can be observed in different nonlinear systems, such as Lorenz system, Rabinovich–Fabrikant system,[28] and memristor system.[29] The traditional transient chaos theory considers that the orbits of a nonlinear system come from the state of chaos firstly and then the transition of orbits would stop in a periodic orbit or a stable point. In other words, the transition of time-domain waveform is from chaos to period or from chaos to a stable point. However, the novel phenomenon of transient chaos is from chaos to period to a stable point, which is founded in this paper. On the other hand, transient period, a new phenomenon different from transient chaos, refers to a system exhibiting periodic orbit firstly and then it converts into chaos at some point. For example, it was firstly reported in Ref. [30] in a memristor-based nonlinear dynamical system with coexisting infinitely many attractors by Bao, who regarded it as an unusual transition behavior. A new 3D chaotic system without equilibrium point but with hidden attractors was proposed in Ref. [12] in which transient period was also found.

Traditional chaotic system was realized by an analog circuit, but there are several problems in the analog circuit, such as component aging, temperature drifting, and voltage changing,[31,32] which has limited the development of the chaotic system. In addition, chaotic the system can be realized by digital signal processing (DSP),[12] advanced RISC machine (ARM),[33] Arduino,[34] and FPGA.[35,36] However, FPGA has advantages compared with DSP, ARM, and Arduino, such as high logic density and versatility.[37]

The contribution of this paper is the finding of a memcapacitive system with stable equilibrium points, multistability, and different kinds of transient transition behaviors. The remaining sections are organized as follows. Section 2 presents the mathematical model of the memcapacitor and analyzes the equilibrium points and stability in the simple memcapacitive system. In Section 3, nonlinear dynamical behaviors are analyzed in the state of self-excited attractors, such as bifurcation diagrams, Lyapunov exponents, coexisting attractors, coexisting bifurcation mode, intermittent chaos, and two different kinds of transient chaos. Section 4 explores the dynamical behaviors of hidden attractors, including Lyapunov exponents, multistability with different initial conditions, transient chaos, and transient period. Finally, FPGA is used to realize the proposed chaotic system in Section 5.

2. The simple memcapacitive system

2.1. Mathematical model of the memcapacitor

The charge-controlled memcapacitive system is described as[38]

$$\begin{cases} V_{\rm c} = C^{-1}(x,q,t)q, \\ \dot{x} = f(x,q,t), \end{cases} \tag{1}$$

where C^{-1} is an inverse memcapacitance, and x is the internal variable of the memcapacitor.

Since C^{-1} and $\dot{x}$ are the functions of x and q, we construct $C^{-1}(x,q,t) = x^2 - c$, $\dot{x} = q^2 - dx - e$. Hence

$$\begin{cases} V_{\rm c} = (x^2 - c)q, \\ \dot{x} = q^2 - dx - e. \end{cases} \tag{2}$$

Assuming the input signal of the memcapacitor is $q = Q_c \sin(2\pi f t)$, the non-transversal pinched hysteresis loop[39] of the memcapacitor can be obtained and shown in Fig. 1, under the condition of $Q_c = 0.6$ C, $f = 0.2$ Hz, $c = 1$, $d = 0.1$, and $e = 0$.

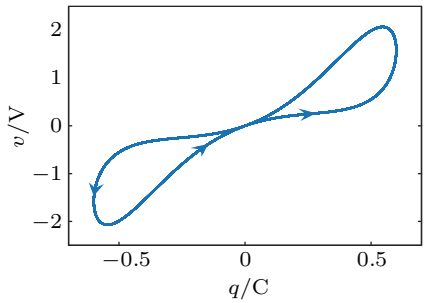


Fig. 1. Non-transversal pinched hysteresis loop.

2.2. The simple memcapacitive system and its equilibrium points and stability

There are three elements in the simple memcapacitive system: a linear resistor, a linear inductor, and a memcapacitor. The circuit schematic diagram is shown in Fig. 2.

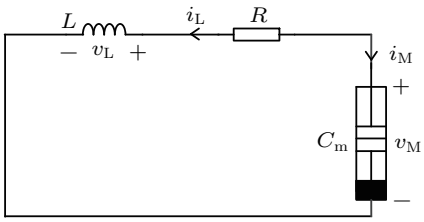


Fig. 2. The circuit schematic diagram of the memcapacitive system.

Based on Kirchhoff's current laws, the following equations can be derived

$$i_{\rm M} = -i_{\rm L}. \tag{3}$$

Hence

$$\frac{{\rm d}q}{{\rm d}t} = i_{\rm M} = -i_{\rm L}. \tag{4}$$

Based on Kirchhoff's voltage laws, we will get

$$v_{\rm M} = v_{\rm L} + Ri_{\rm L}. \tag{5}$$

Thus

$$\frac{\mathrm{d}i_{\mathrm{L}}}{\mathrm{d}t}=\frac{1}{L}(-Ri_{\mathrm{L}}+v_{\mathrm{M}}). \tag{6}$$

So far, according to Eqs. (2), (4), and (6), the equations of the system can be presented as follows:

$$\begin{cases}\dfrac{\mathrm{d}q}{\mathrm{d}t}=-i_{\mathrm{L}},\\ \dfrac{\mathrm{d}i_{\mathrm{L}}}{\mathrm{d}t}=\dfrac{1}{L}(-Ri_{\mathrm{L}}+(x^2-c)q),\\ \dfrac{\mathrm{d}x}{\mathrm{d}t}=q^2-dx-e.\end{cases} \tag{7}$$

By allowing $\dot{x}=\mathrm{d}q/\mathrm{d}t$, $\dot{y}=\mathrm{d}i_L/\mathrm{d}t$, $\dot{z}=\mathrm{d}x/\mathrm{d}t$, and setting $1/L=a$ and $R=b$, the dimensionless equations can be described as

$$\begin{cases}\dot{x}=-y,\\ \dot{y}=a(-by+(z^2-c)x),\\ \dot{z}=x^2-dz-e.\end{cases} \tag{8}$$

Let $\dot{x}=\dot{y}=\dot{z}=0$, if $a=1$ and $e=0$, we will get three equilibrium points: $S_0=(0,0,0)$, $S_+=(X,0,Z)$, $S_-=(-X,0,Z)$, $Z=c^{1/2}$, $X^2=dZ$.

The Jacobian matrix of the system (8) is given as

$$\boldsymbol{J}=\begin{bmatrix}0 & -1 & 0\\ z^2-c & -b & 2xz\\ 2x & 0 & -d\end{bmatrix}. \tag{9}$$

The characteristic equation is yielded as

$$f(\lambda)=\lambda(\lambda+b)(\lambda+d)-(c-z^2)(\lambda+d)+4x^2z. \tag{10}$$

Substituting S_+ and S_- into Eq. (10), then we will gain

$$\begin{aligned}f(\lambda)&=\lambda(\lambda+b)(\lambda+d)+4dc\\ &=\lambda^3+(b+d)\lambda^2+bd\lambda+4dc.\end{aligned} \tag{11}$$

Thus, we will obtain the following characteristic equation

$$\det(\lambda\boldsymbol{I}-\boldsymbol{J})=\lambda^3+a_1\lambda^2+a_2\lambda+a_3=0, \tag{12}$$

where

$$\begin{cases}a_1=b+d,\\ a_2=bd,\\ a_3=4dc.\end{cases} \tag{13}$$

It is easy for us to gain the Routh array shown in expression (14)

$$\begin{array}{ccc}\lambda^3 & 1 & bd\\ \lambda^2 & b+d & 4dc\\ \lambda^1 & (b+d)bd-4dc & 0\\ \lambda^0 & 4dc & 0\end{array} \tag{14}$$

Then, the real parts of the roots of system (8) are negative if and only if

$$\begin{cases}b+d>0,\\ (b+d)bd-4dc>0,\\ 4dc>0.\end{cases} \tag{15}$$

As a result, when

$$\begin{cases}b>0,\\ c>0,\\ d>0,\\ c<0.25b(b+d),\end{cases} \tag{16}$$

the condition of expression (15) will be satisfied for two nonzero equilibrium points.

Thus, we will get the following conclusion. The two nonzero equilibrium points are unstable when $c>0.25b(b+d)$, stable when $c<0.25b(b+d)$.

3. Coexisting self-excited attractors

3.1. Bifurcation diagram of the state variable z with the changing of c

Substituting $a=1$, $b=1.3$, $d=0.1$, and $e=0$ in system (8), two equilibrium points in the memcapacitive system are unstable when $c>0.25b(b+d)=0.455$, stable when $c<0.25b(b+d)=0.455$. Thus, the critical parameter between stable and unstable equilibrium points is given as $c_{\mathrm{critical}}=0.455$.

When the initial condition is chosen as (0.1, 0.1, 0.1), the bifurcation diagram and Lyapunov exponents are plotted in Fig. 3. In the bifurcation diagram, y is chosen as state variable and $x=0.4$ is chosen as Poincare plane. In Fig. 3(b), the dynamics of the system described by three Lyapunov exponents are consistent well with that in the bifurcation diagram.

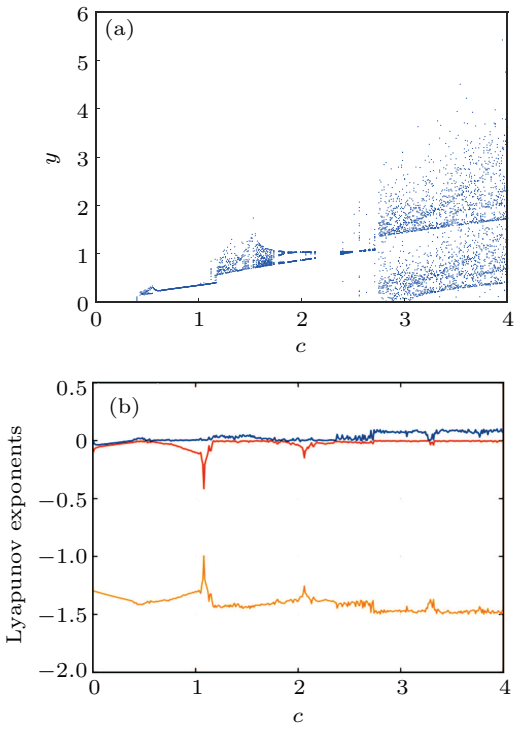


Fig. 3. Bifurcation diagram and Lyapunov exponents with respect to c. (a) Bifurcation diagram of y, (b) Lyapunov exponents.

When $0<c<0.44$, three Lyapunov exponents are negative, and the memcapacitive system shows a point attrac-

tor as shown in Fig. 4(a) with $c = 0.4$. In the region of $0.44 < c < 0.6$, which is the first chaotic region in the bifurcation diagram, chaotic attractors are plotted in Fig. 4(b) with $c = 0.5$. With the increasing of c, three Lyapunov exponents are calculated as $LE_1 = 0$, $LE_2 < 0$, and $LE_3 < 0$. So, the system displays periodic behavior with parameter c changing from 0.6 to 1.17, and the limit cycle is given in Fig. 4(c) with $c = 1$. When $1.17 < c < 1.7$, the second chaotic region of the system can be found. The phase diagram is shown in Fig. 4(d) with $c = 1.5$. In the region of $1.7 < c < 2.75$, the system shows periodic behavior. There is a small blank area, in which the phenomenon of coexisting bifurcation mode can be found, in the region of $2.14 < c < 2.37$ in Fig. 3(a). The blank area is caused by the selection of the Poincare plane. In Fig. 3(a), $x = 0.4$ is chosen as the Poincare plane and z is chosen as state variable. With further increase of c, the third chaotic area is manifested in the region of $2.75 < c < 4$. The dynamic behaviors of memcapacitive chaotic system for parameter c are shown in Table 1.

Table 1. Dynamic behaviors of memcapacitive chaotic system for parameter c.

Parameter ranges	Dynamical behaviors
$0 < c < 0.44$	Point attractor
$0.44 < c < 0.6$	Chaotic attractor
$0.6 < c < 1.17$	Limit cycle
$1.17 < c < 1.7$	Chaotic attractor
$1.7 < c < 2.75$	Periodic behavior
$2.75 < c < 4$	Chaotic attractor

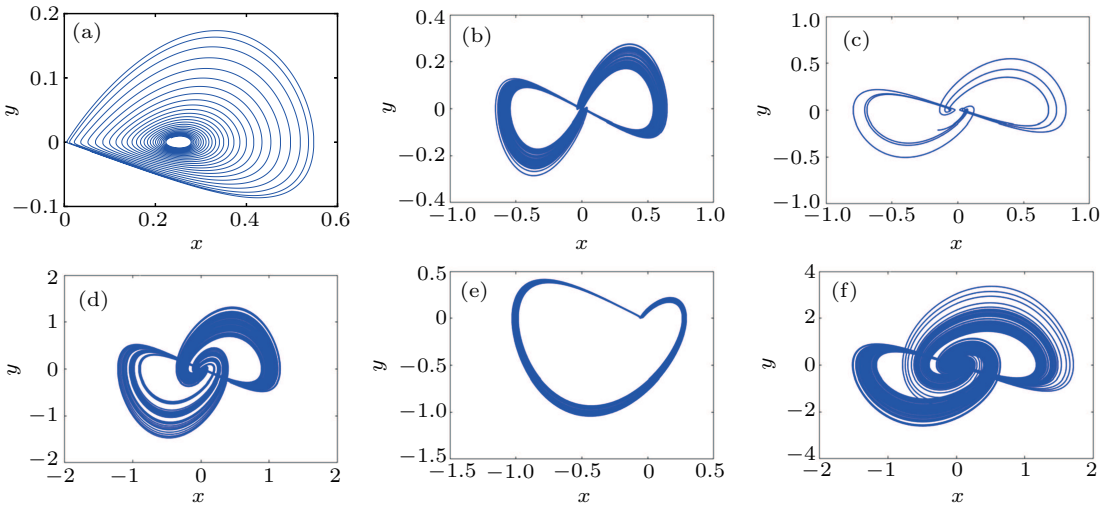


Fig. 4. Phase diagrams in x–y plane with respect to c: (a) $c = 0.4$, (b) $c = 0.5$, (c) $c = 1$, (d) $c = 1.5$, (e) $c = 2.2$, (f) $c = 3$.

3.2. Coexisting attractors and coexisting bifurcation mode

When $a = 1$, $b = 1.3$, $d = 0.1$, and $e = 0$, and c varies from 0.6 to 3, coexisting self-excited attractors are shown in Fig. 5. The trajectories colored in red start from the initial condition of $x(0) = 0$, $y(0) = 1$, $z(0) = 1$, and in blue come from $x(0) = 0$, $y(0) = -1$, $z(0) = 1$.

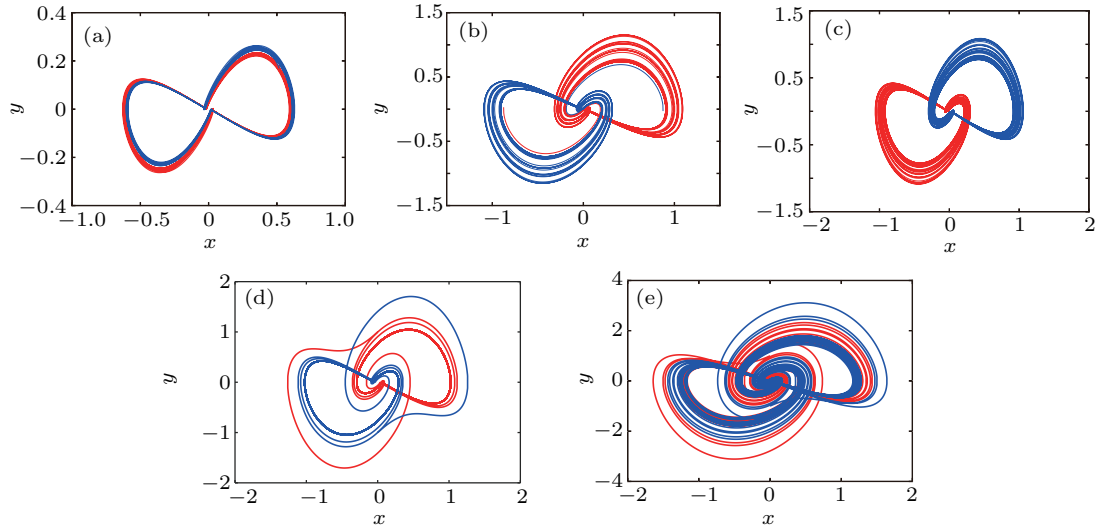


Fig. 5. Coexisting self-excited attractors in the x–y plane with respect to c under initial conditions of $(0, -1, 1)$ (blue) and $(0, 1, 1)$ (red): (a) $c = 0.6$, (b) $c = 1.6$, (c) $c = 1.7$, (d) $c = 2.5$, (e) $c = 3$.

When $c = 0.6$, the coexistence of quasiperiodic attractors is shown in Fig. 5(a). Figure 5(d) shows the coexistence of two periodic attractors. The chaotic attractors are displayed in Fig. 5(b), Fig. 5(c), and Fig. 5(e).

The phenomenon of coexisting bifurcation shown in the small blank area is shown in Fig. 3(a), and the bifurcation diagram of coexisting bifurcation behavior is shown in Fig. 6. The coexisting bifurcation mode is caused by different initial conditions with the same system parameters. In Fig. 6, x is chosen as state variable with parameter c varying from 2 to 4. The trajectories colored with red come from the initial condition of (0.1, −0.5, 0.1), and that colored with blue come from the initial condition of (0.1, 0.5, 0.1). Phase diagrams under coexisting bifurcation mode with $c = 2.1$ and $c = 2.4$ are shown in Fig. 7(a) and Fig. 7(b).

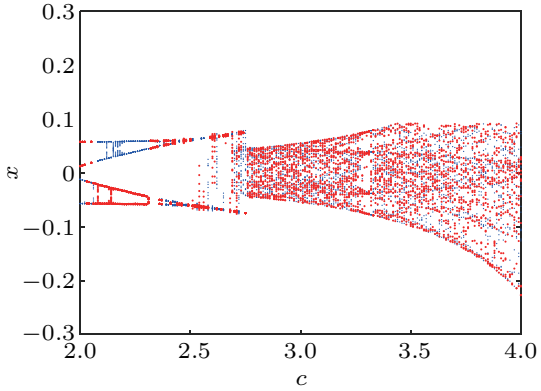


Fig. 6. Coexisting bifurcation mode under initial conditions of (0.1, 0.5, 0.1) (blue) and (0.1, −0.5, 0.1) (red).

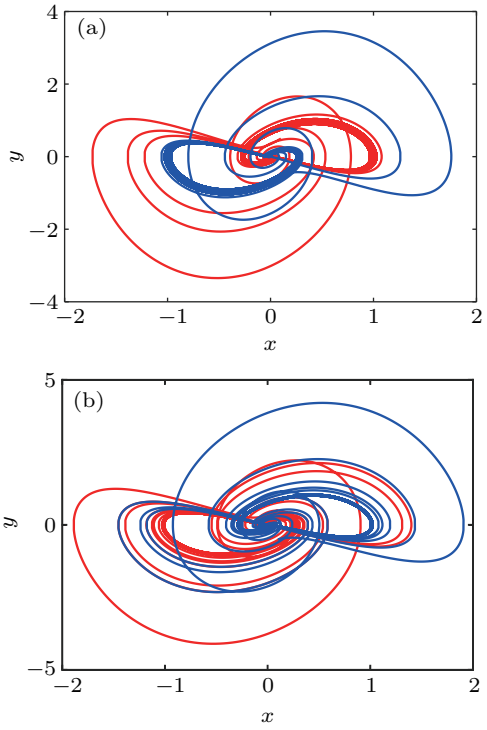


Fig. 7. Phase diagrams under the coexisting bifurcation mode (a) $c = 2.1$, (b) $c = 2.4$.

3.3. Multistability depends on initial states of $x(0)$ and $z(0)$

In system (8), the parameters are taken as $a = 1$, $b = 1.3$, $c = 3.3$, $d = 0.1$, and $e = 0$ and the initial states are chosen as $(x(0), 0, 2)$ and $(-0.5, 0, z(0))$ in Fig. 8(a) and Fig. 8(b) separately. The bifurcation diagrams of state variables x and z varying with $x(0)$ and $z(0)$ are shown in Fig. 8(a) and Fig. 8(b).

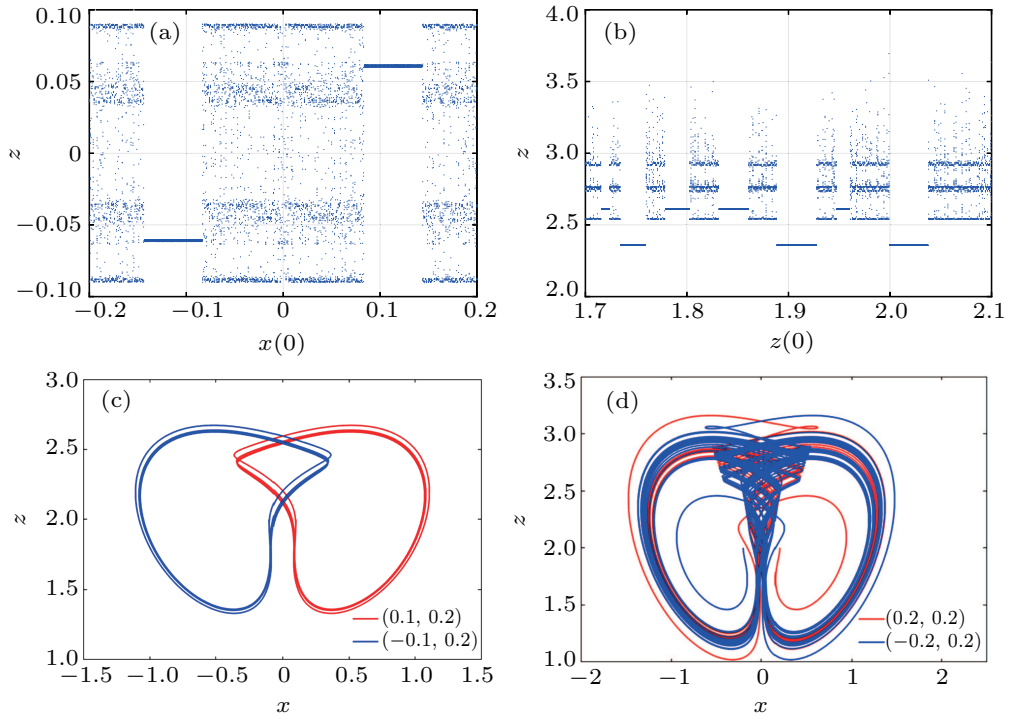


Fig. 8. Multistability with respect to $x(0)$ and $z(0)$: (a) bifurcation diagram with respect to $x(0)$, (b) bifurcation diagram with respect to $z(0)$, (c) coexisting periodic attractors, (d) coexisting chaotic attractors.

In Fig. 8(a), the periodic regions lie in intervals $(-0.14, -0.09)$ and (0.09, 0.14). The memcapacitive system displays coexisting periodic attractors in x–z plane with respect to initial state $(\pm 0.1, 0, 2)$. The chaotic regions lie in intervals $(-0.2, -0.14)$, $(-0.09, 0.09)$, and (0.14, 0.2), in which coexisting chaotic attractors appear with respect to initial state ($\pm$ 0.2, 0, 2). Coexisting periodic attractors and chaotic attractors are shown in Fig. 8(c) and Fig. 8(d) separately.

3.4. Intermittent chaos and transient chaos

Transient chaos theory considers that the orbits of a nonlinear system come from the state of chaos firstly and then the transition of orbits would stop in a periodic orbit or a stable point. Intermittency is the irregular alternation of periodic and chaotic dynamics of chaotic system. Intermittent chaos and transient chaos could be determined in periodic window.[22] In a periodic window, transient chaos is caused by a nonattracting chaotic set, while intermittent chaos caused by an interior crisis. The crisis refers to sudden changes in the chaotic attractor when the system parameter is varied. Crises in the chaotic system could be divided into two types, boundary crises, and interior crises. When the chaotic attractor moves to the unstable orbit of the boundary, an attracting chaotic set would change into a nonattracting chaotic set. Transient chaos lies in the nonattracting chaotic set. This phenomenon is called boundary crisis. Interior crisis is the phenomenon that a chaotic attractor moves to a nonattracting chaotic set. After that, a smaller chaotic attractor becomes a larger one.

In Fig. 9, when we choose x as state variable, the initial condition as (0.1, 0.1, 0.1), $c = 3.3$ in system (8), intermittent chaos can be found in the proposed system. Figure 9(a) shows the time-domain waveform of state variable x, which alternates between chaotic regions and periodic regions. The chaotic regions in blue lie in three intervals: (1, 100), (1050, 1550), (3400, 3600); the periodic regions in red lie in others: $(100, 1050)$, (1550, 3400), (3600, 5000). Chaos-1 and p-1, chaos-2 and p-2, chaos-3 and p-3 are shown in Fig. 9(b), Fig. 9(c), and Fig. 9(d) separately.

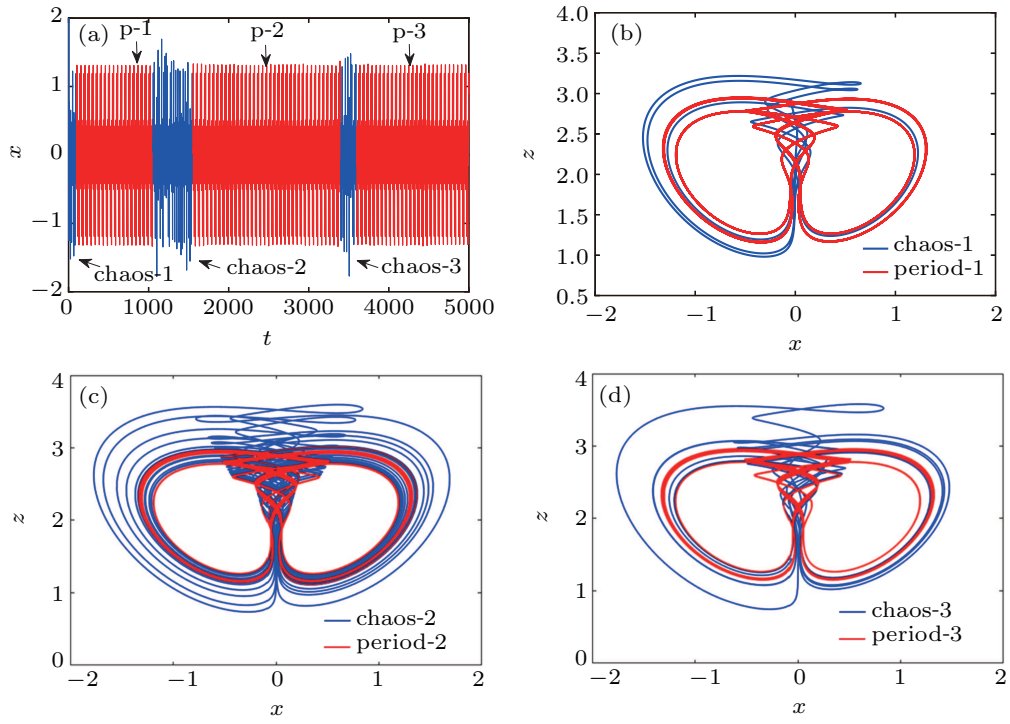


Fig. 9. Intermittent chaos (a) time-domain waveform, (b) chaos-1 and p-1, (c) chaos-2 and p-2, (d) chaos-3 and p-3.

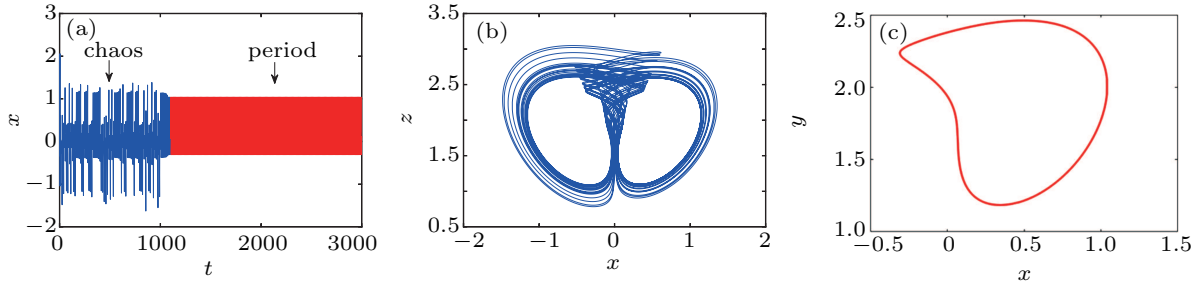


Fig. 10. Transient chaos from chaos to period (a) time-domain waveform, (b) chaotic attractor when $0 < t < 1000$, (c) periodic attractor when $1500 < t < 3000$.

Two different kinds of transient chaos can be found in the self-excited system. The first transient chaos is from chaos to period. When setting parameters $a = 1$, $b = 1.3$, $c = 2.76$, $d = 0.1$, and $e = 0$ with the initial condition (0.1, 0.1, 0.1), the system displays chaos firstly and then switches over to periodic state in Fig. 10(a). Chaotic attractor and periodic attractor are shown in Figs. 10(b) and 10(c) separately.

The second transient chaos is a novel phenomenon. When parameters $a = 1$, $b = 1.3$, $c = 1.5$, $d = 0.1$, and $e = -0.4$, the initial condition is set as $(-0.2, 3, -2)$. In Fig. 11(a), with the increase of the time, it is found that the evolution of the orbits is from chaos to period to chaos to stable point, which is different from ordinary transient chaos phenomenon. The system exhibits chaos-1 initially and then switches over to periodic oscillations. After that, it exhibits chaos-2. Finally, the trajectories change into a stable point. Phase diagrams in x–z plane of chaos-1 and period, chaos-2 and stable point are shown in Figs. 11(b) and 11(c) separately.

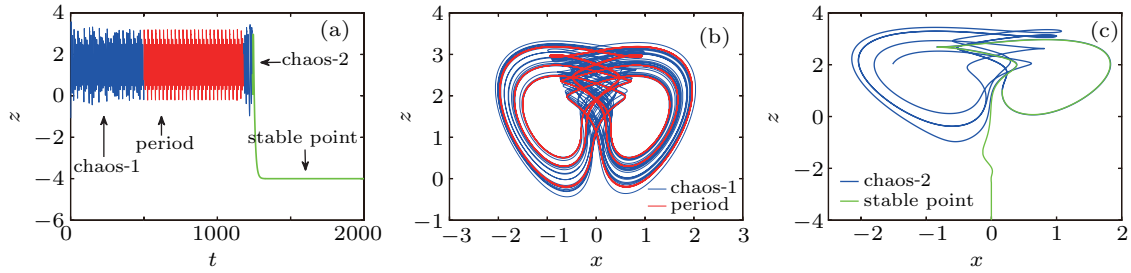


Fig. 11. Transient chaos from chaos to period to chaos to stable point: (a) process of evolution with timescale, (b) chaos-1 and period, (c) chaos-2 and stable point.

4. Hidden attractors

4.1. Hidden attractors with two stable equilibrium points

4.1.1. Hidden chaotic system and its dynamic behavior analysis

Definition 1[40–43] An attractor is called a self-excited attractor if its basin of attraction intersects with any open neighborhood of an equilibrium; otherwise it is called a hidden attractor

Substitute $a = 1$, $b = 1.3$, $c = 0.437$, $d = 0.1$, and $e = 0$ in Eq. (10) and let $\dot{x} = \dot{y} = \dot{z} = 0$. Thus, three equilibrium points are calculated as follows: $S_0 = (0,0,0)$, $S_+ = (0.2575, 0, 0.6633)$, $S_- = (-0.2575, 0, 0.6633)$. On the one hand, the eigenvalue of S_0 is calculated as $\lambda_1 = -1.5771$, $\lambda_2 = -0.1$, and $\lambda_3 = 0.2771$, so the equilibrium S_0 is unstable. On the other hand, the same eigenvalues of S_+ and S_- are calculated as $\lambda_1' = -1.3971$ and $\lambda_{2,3}' = -0.0014 \pm 0.3549\mathrm{i}$, so they are saddle points.

As indicated in Ref. [43], hidden chaotic attractors are presented in a generalized Lorenz system of fractional order with an unstable point and two saddle points. In order to verify that the memcapacitive system has hidden attractors, the existence of small neighborhood of the unstable equilibrium S_0, from which orbits are all attracted by the stable equilibriums S_+ or S_-, should be verified. As shown in Fig. 12(a), orbits which are starting from small neighborhood of S_0 either tend to S_+ or S_-. In Fig. 12(b), 50 random points are chosen to represent the source of the orbits (either to S_+ (red) or S_- (blue)). The big sphere with (0, 0, 0) center and 0.015 radius is chosen to represent the small neighborhood.

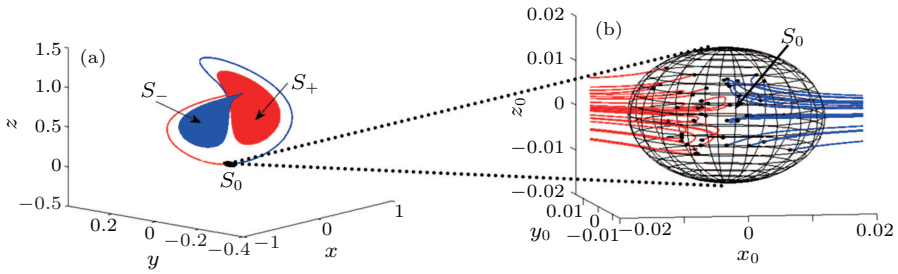


Fig. 12. Existence of small neighborhood of S_0 (a) orbits attracted by the stable equilibriums S_+ or S_-, (b) small neighborhood of S_0.

4.1.2. Multistability with different initial conditions

The multistability of the hidden attractors refers to different attractors in different initial conditions with fixed parameters. In Fig. 13, we choose the parameters as $a = 1$, $b = 1.3$, $c = 0.44$, $d = 0.1$, and $e = 0$, the initial condition as $(x_0, y_0) = (0.1, 0.2)$. We just change the initial variable z_0 to get different hidden attractors. The hidden attractors are divided in different regions with the increase of z_0, which is found in Fig. 13. For example, when $z_0 = -5$, $z_0 = -1$, $z_0 = 0$, and $z_0 = 2$, the system displays hidden attractors. But it is stable point in lift plane when $z_0 = -2.5$ and $z_0 = 1$, stable point in right plane when $z_0 = -2$ and $z_0 = -0.5$.

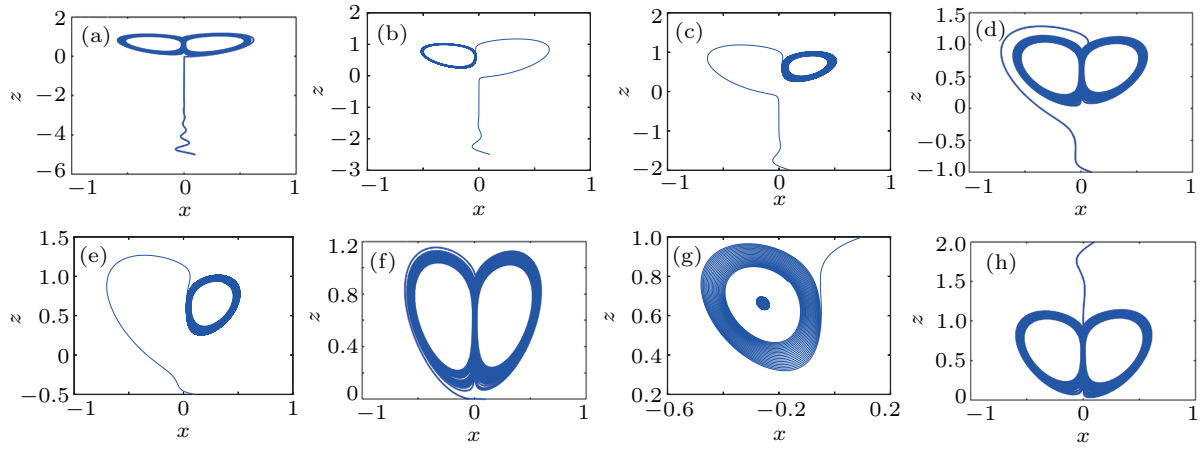


Fig. 13. Phase diagrams of chaotic system in different initial conditions with the changing of z_0: (a) $z_0 = -5$, (b) $z_0 = -2.5$, (c) $z_0 = -2$, (d) $z_0 = -1$, (e) $z_0 = -0.5$, (f) $z_0 = 0$, (g) $z_0 = 1$, and (h) $z_0 = 2$.

4.2. Transient chaos and transient period

In hidden chaotic system, when setting parameters as $a = 1$, $b = 1.3$, $c = 0.435$, $d = 0.1$, and $e = 0$, the initial condition as $(0, -1.5, 0)$, the time-domain waveform of state variable x is shown in Fig. 14(a). This phenomenon of transient chaos is from chaos to stable point. The system exhibits chaos initially and then switches over to a stable point. Phase diagram in x–z plane of transient chaos is shown in Fig. 14(b).

When setting parameters as $a = 1$, $b = 1.3$, $c = 0.44$, $d = 0.1$, and $e = 0$, the initial condition as $(0.1, -0.1, 0.7)$, the time-domain waveform of state variable x is shown in Fig. 14(c). This phenomenon of transient period is from period to chaos. The system exhibits periodic oscillation initially and then switches over to chaos oscillation. Phase diagram in x–z plane of transient period is shown in Fig. 14(d).

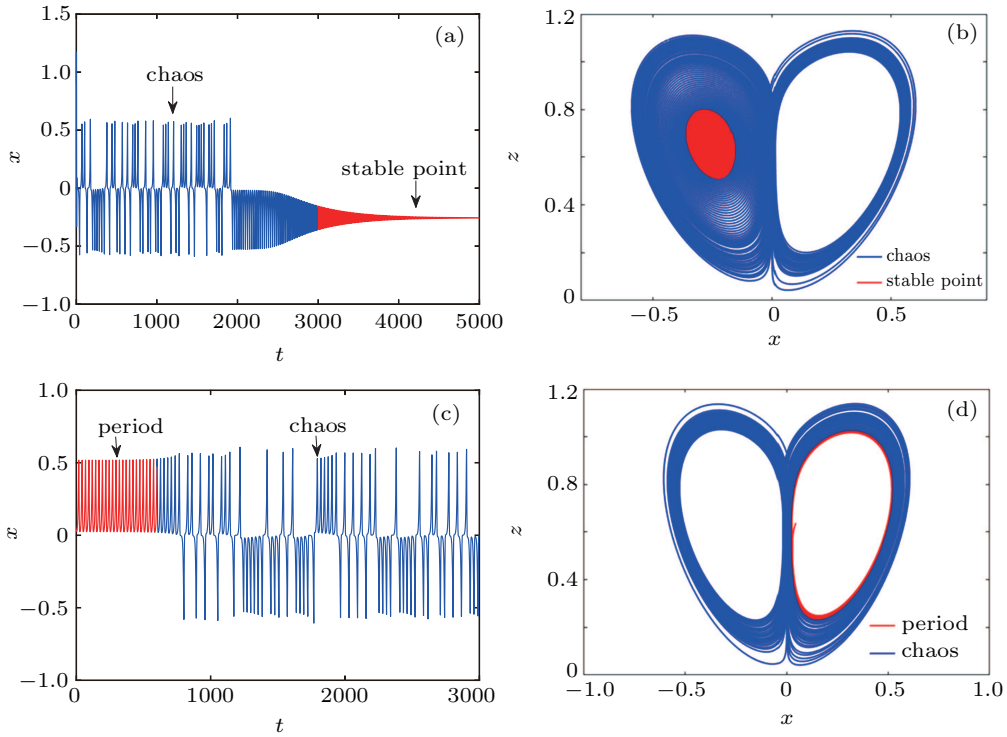


Fig. 14. Transient chaos and transient period (a) transient chaos from chaos to stable point, (b) x–z plane of transient chaos, (c) transient period from period to chaos, (d) x–z plane of transient period.

5. FPGA implementation of the chaotic system

In recent years, many chaotic systems are realized by field programmable gate array (FPGA) in academic circles.[32,34,44–46] So, it is a growing tendency that a chaotic system will be implemented by FPGA technology. As a result, in this paper, the FPGA technology is used to realize the chaotic system.

Our FPGA development board is AC620, which includes

main chip EP4CE10F17C8 N. In addition, digital to analog converter chip is ACM9767, which is connected with the oscilloscope. In FPGA, the second-order Runge–Kutta algorithm is used to realize the chaotic system.

Setting $a=1$, $b=1.3$, $d=0.1$, $e=0$, and $h=1/128$, the memcapacitive system is discretized as

$$\begin{cases} x_{k+1/2} = x_k + \dfrac{h}{2}(-y_k), \\ y_{k+1/2} = y_k + \dfrac{h}{2}a(-by_k + (z_k^2 - c)x_k), \\ z_{k+1/2} = z_k + \dfrac{h}{2}(x_k^2 - dz_k - e), \end{cases} \tag{17}$$

$$\begin{cases} x_{k+1} = x_k + h(-y_{k+1/2}), \\ y_{k+1} = y_k + ha(-by_{k+1/2} + (z_k^2 - c)x_k), \\ z_{k+1} = z_k + h(x_{k+1/2}^2 - dz_{k+1/2} - e). \end{cases} \tag{18}$$

The state machine flowchart of the system is shown in Fig. 15(a). The phase diagram of FPGA experiment is shown in Fig. 15(b). One can see that the phase diagram in FPGA experiment is identical to that in Fig. 5(c).

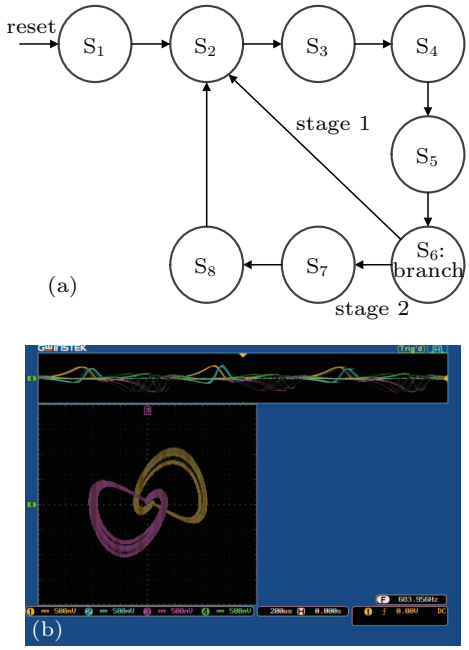


Fig. 15. FPGA implementation (a) state machine flowchart, (b) phase diagram.

S_1: Initialize the values of register variables in the circuit;

S_2: Calculate z^2, x^2, ry, nx, bz, and move y 26 bits to the left;

S_3: Calculate xz^2 and move y, ry, nx, bz, x^2 26 bits to the left;

S_4: Calculate $xz^2 - ry - nx$, $x^2 - bz$;

S_5: Change the bits of calculation results into 32 bits;

S_6: If in stage 1, implement the operation in system (17); direct to state S_1. If in stage 2, implement the operation in system (18); direct to state S_7;

S_7: Add offset;

S_8: Change the bits of calculation results into 14 bits.

6. Conclusion

In this paper, hidden and self-excited attractors are studied in a simple memcapacitive system. First, the critical parameter between self-excited attractor and hidden attractor is obtained by the calculation of equilibrium points and stability. In addition, there are only three elements in the system, but the system has complex chaotic dynamical behaviors, such as coexisting attractors, hidden attractors, coexisting bifurcation modes, intermittent chaos, and multistability. What is more, four different kinds of transient transition behaviors are found in this system: chaos to period, chaos to a stable point, chaos to period to a stable point, and period to chaos.

References

[1] Lorenz E N 1963 *J. Atmos. Sci.* **20** 130
[2] Rössler 1976 *Phys. Lett. A.* **57** 397
[3] Chen G and Ueta T 1999 *Int. J. Bifur. Chaos* **9** 1465
[4] Lü J and Chen G 2002 *Int. J. Bifur. Chaos* **12** 659
[5] Chua L O and Lin G N 1990 *IEEE Trans. Circuits Syst.* **37** 885
[6] Liu C, Liu L, Liu T and Li P 2004 *Chaos Solitons Fractals* **22** 1031
[7] Kuznetsov N V, Leonov G A and Vagaitsev S 2010 *IFAC Proc.* **43** 29
[8] Dudkowski D, Jafari S, Kapitaniak T, Kuznetsov N V, Lwonov G A and Prasad A 2016 *Phys. Rep.* **637** 1
[9] Kuznetsov N and Leonov G 2014 *IFAC Proc.* **47** 5445
[10] Liu Y F, Yang D D, Wang L X and Li Q 2018 *Chin. Phys. Lett.* **35** 046801
[11] Jia M M, Jiang H G and Li W J 2019 *Acta Phys. Sin.* **68** 130503 (in Chinese)
[12] Zhou W, Wang G, Shen Y, Yuan F and Yu S 2018 *Int. J. Bifur. Chaos* **28** 1830033
[13] Pham V T, Jafari S, Kapitaniak T, Volos C and Kingni S T 2017 *Int. J. Bifur. Chaos* **27** 1750053
[14] Sprott J C, Wang X and Chen G 2013 *Int. J. Bifur. Chaos* **23** 1350093
[15] Barati K, Jafari S, Sprott J C and Pham V T 2016 *Int. J. Bifur. Chaos* **26** 1630034
[16] Lai Q, Akgul A, Zhao X W and Pei H 2017 *Int. J. Bifur. Chaos* **27** 1750142
[17] Pham V T, Volos C, Jafari S and Kapitaniak T 2017 *Nonlinear Dyn.* **87** 2001
[18] Wei Z, Moroz I, Sprott J C, Akgul A S and Zhang W 2017 *Chaos* **27** 033101
[19] Wang G, Shi C, Wang X and Yuan F 2017 *Math. Probl. Eng.* **2017** 6504969
[20] Yuan F, Wang G, Shen Y and Wang X 2016 *Nonlinear Dyn.* **86** 37
[21] Mou J, Sun K, Ruan J and He S 2016 *Nonlinear Dyn.* **86** 1735
[22] Lai Y C and Tél T 2011 *Transient chaos: complex dynamics on finite time scales*, Vol. 173 (New York: Springer) pp. 1–103
[23] Croquette V and Poitou C 1981 *J. Physique Lett.* **42** 1353
[24] Arecchi F T, Meucci R, Puccioni G and Tredicce J 1982 *Phys. Rev. Lett.* **49** 1217
[25] Arecchi F T and Lisi F 1983 *Phys. Rev. Lett.* **50** 1330
[26] Sathiyadevi K, Karthiga S, Chandrasekar V K, Senthilkumar D V and Lakshmanan M 2019 *Commun. Nonlinear Sci. Numer. Simul.* **72** 586
[27] Maslennikov O V, Nekorkin V I and Jürgen K 2018 *Chaos* **28** 033107
[28] Danca M F 2016 *Nonlinear Dyn.* **86** 1263
[29] Bao B C, Jiang P, Wu H G and Hu F W 2015 *Nonlinear Dyn.* **79** 2333
[30] Bao H, Wang L, Bao B C and Wang G Y 2018 *Commun. Nonlinear Sci. Numer. Simul.* **57** 264
[31] Dong E Z, Yuan M F, Zhang C, Tong J G, Chen Z Q and Du S Z 2018 *Int. J. Bifur. Chaos* **28** 1850081
[32] Jia H, Guo Z, Wang S and Chen Z 2018 *Int. J. Bifur. Chaos* **28** 1850161

[33] Elkholy M M, Elkholy H M E and Elkouny A 2016 *IEEE Procedding of 10th International Conference on Computer Engineering & Systems (ICCES)*, December 23–24, 2015, Cairo, EGYPT pp. 81–85

[34] Mauricio Z D L H, Leonardo A and Yolanda V 2015 *Sci. World J.* **2015** 1

[35] Rajagopal K, Panahi S, Karthikeyan A, Alsaedi A, Pham V T and Hayat T 2018 *Int. J. Bifur. Chaos* **28** 1850164

[36] Dong E Z, Wang Z, Yu X, Chen Z Q and Wang Z H 2018 *Chin. Phys. B* **27** 010503

[37] Dong E Z, Liang Z H, Du S Z and Chen Z Q 2016 *Nonlinear Dyn.* **83** 623

[38] Di Ventra M, Pershin Y V and Chua L O 2009 *Proc. IEEE* **97** 1717

[39] Adhikari S P, Sah M P, Kim H and Chua L O 2013 *IEEE Trans. Circuits Syst. I-Regul. Paper* **60** 3008

[40] Leonov G A, Kuznetsov N V and Vagaitsev V I 2012 *Physica D* **241** 1482

[41] Leonov G A, Kuznetsov N V and Mokaev T 2015 *Eur. Phys. J. Spec. Top.* **224** 1421

[42] Leonov G A and Kuznetsov N V 2013 *Int. J. Bifurc. Chaos* **23** 1330002

[43] Dance M 2017 *Nonlinear Dyn.* **89** 577

[44] Rajagopal K, Guessas L, Vaidyanathan S, Karthikeyan A and Srinivasan A 2017 *Math. Probl. Eng.* **2017** 7307452

[45] Rajagopal K, Jafari S and Laarem G 2017 *Pramana - J. Phys.* **89** 92

[46] Li C, Sprott J C, Liu Y, Gu Z and Zhang J 2018 *Int. J. Bifur. Chaos* **28** 1850163